

Effect of Temperature on Nylon 6 Fibers at Different Denier Values and Study of Macromolecular Parameters by SAXS Technique

N. PRASAD,¹ J. PATNAIK,¹ N. BOHIDAR,² T. MISHRA³

¹ Department of Physics, Ranchi University, Ranchi, India PIN-834008

² Department of Chemistry, Women's College, Sambalpur-768001, India

³ R.I.T., Kalunga-770031, Orissa, India

Received 13 July 1995; accepted 14 December 1996

ABSTRACT: Small-angle X-ray scattering (SAXS) was used to evaluate various macromolecular parameters of Nylon 6 textile fiber at denier values of 15/1, 18/1, and 20/1 treated at different temperatures within the range of 20–63°C. The theories of Kratky, Porod, Bueche, and Wendorff were applied to the densely packed two-phase system of Nylon 6, which conforms to the general micelle system. The values determined for the parameters, such as microvoid dimensions (d), the void percentage (w_1), the length of coherence (lc), the specific inner surface (o/v), and the transversal lengths (l_1 and l_2) of Nylon 6 fiber at a denier value of (15/1) at temperature 38°C are 62.5 Å, 0.0181%, 480.55 Å, $3.214 \times 10^{-6} \text{ Å}^{-1}$, and 225 Å and $1244 \times 10^3 \text{ Å}$, respectively. A comparative study of the above parameters at different temperatures was also made and a correlation was established. © 1998 John Wiley & Sons, Inc. *J Appl Polym Sci* **67**: 1753–1759, 1998

INTRODUCTION

The theory^{1,2} and the technique^{3,4} of small-angle X-ray scattering were considered to be useful for investigating the structural parameters of semi-crystalline polymers like Nylon 6 fibers, where the scattering is due to the heterogeneity of electron densities in crystalline and amorphous phases. The macromolecular parameters of a densely packed two-phase system can be derived from the characteristics of the scattering curves after the theories of Kratky.⁵

Although various macromolecular parameters of naturally occurring textile fibers like silk⁶ and tussar⁷ have been reported, little attention has been paid to the detailed investigation of macromolecular parameters of Nylon 6 fiber with differ-

ent denier/filament values as well as at different temperatures. Hence, in the present study, an attempt was made to study the effect of temperature on the macromolecular parameters. The SAXS technique was used by taking into consideration the theories of Porod,⁸ Debye and Bueche,¹ Kratky,⁹ and Wendorff.¹⁰

EXPERIMENTAL AND THEORY

The desmeared intensity data were obtained from the smeared intensity data recorded from a line source Matchlett A-2 X-ray diffraction tube with a Cu target. The X-ray unit was run at 50 kV and 50 mA. The SAXS camera after Kratky¹¹ is capable of recording the scattering intensities down to an angle of the order 10^{-4} rad corresponding to a Bragg value of 10,000 Å. The collimating system is a slit of width 120 μm and is free from

Correspondence to: N. Bohidar.

Journal of Applied Polymer Science, Vol. 67, 1753–1759 (1998)
© 1998 John Wiley & Sons, Inc. CCC 0021-8995/98/101753-07

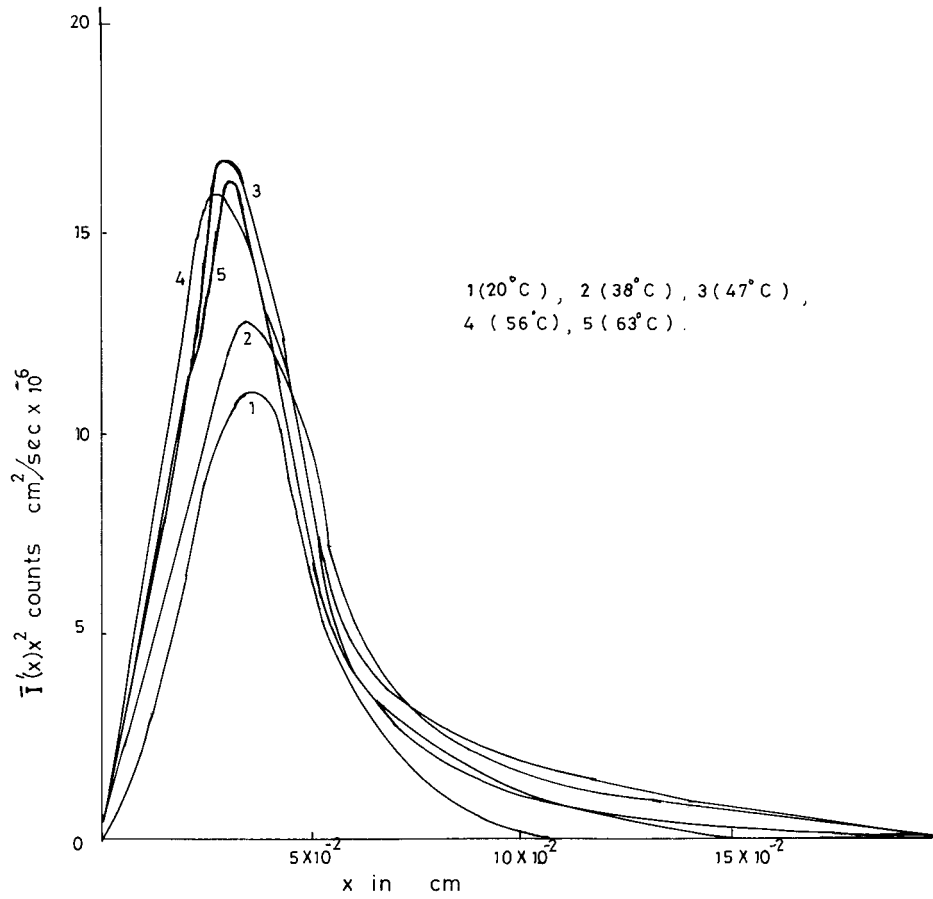


Figure 1 Comparative plots for invariant Q with normalized intensity, \bar{I} .

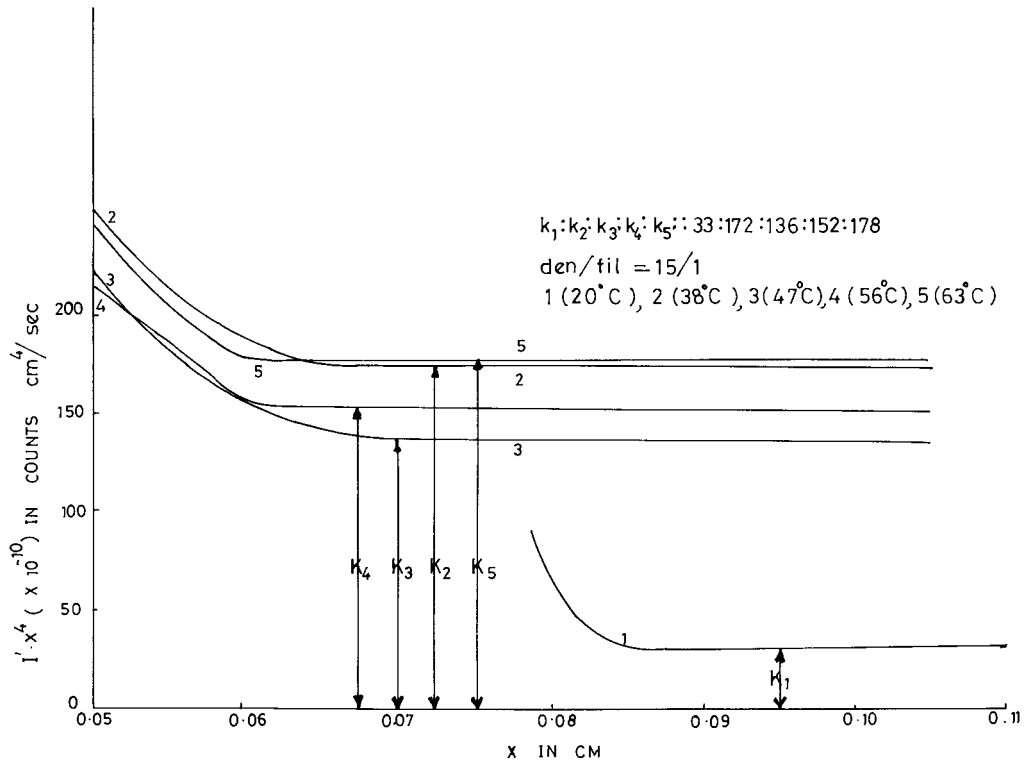


Figure 2 Comparative plots of run constant with normalized intensity.

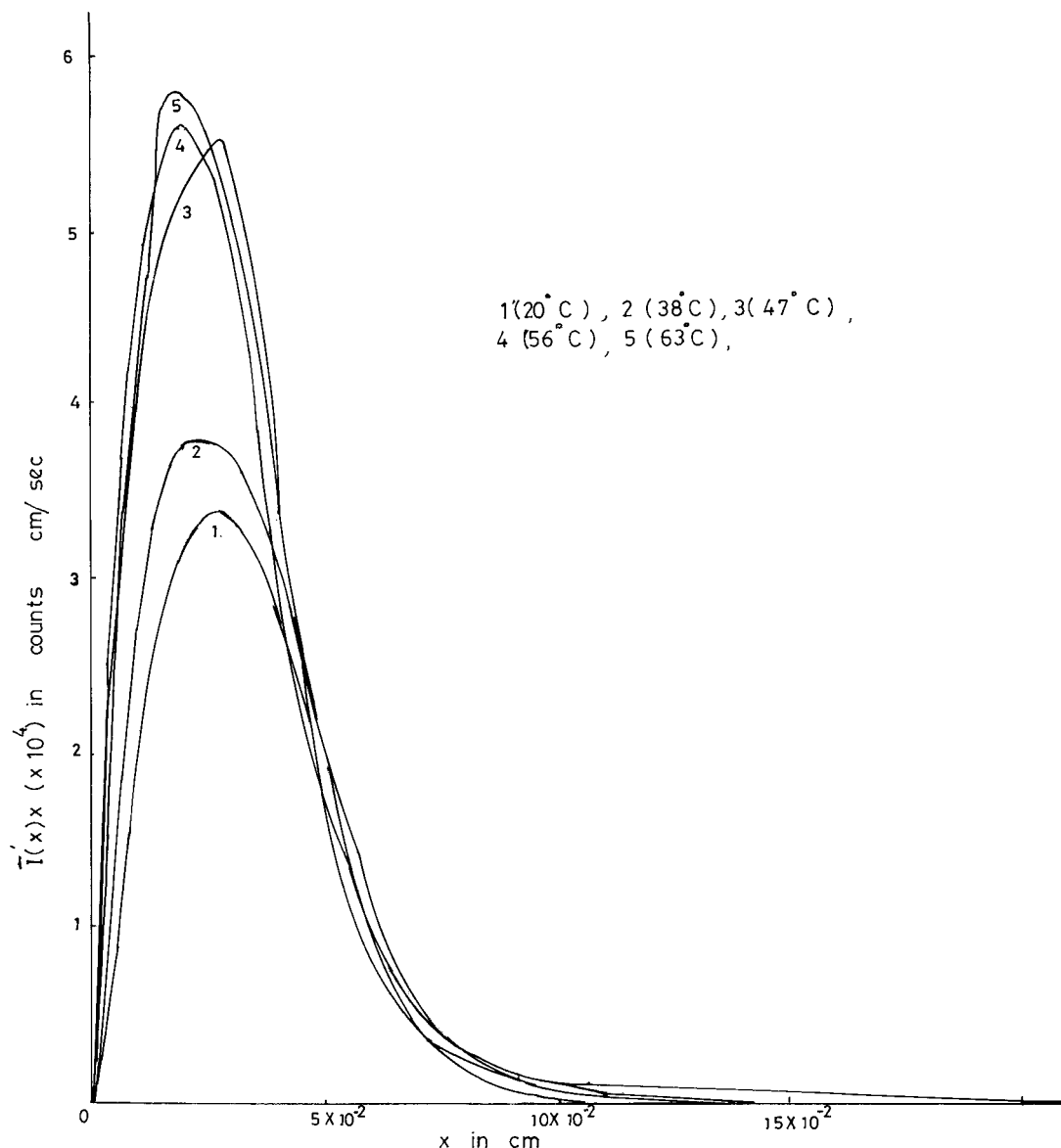


Figure 3 Comparative plot of the integrated energy E with normalized intensity \bar{I} .

parasitic scattering. The yarn sample of Nylon 6 was taken in a Mark capillary tube of diameter 0.1 cm, having negligible scattering. The scattering due to air present between the sample and the detector was avoided by evacuating the space to a value equal to 5×10^{-3} Torr. Scattering intensities were determined by a proportional counter attached to an electronically maintained automatic step-scanner device.

The intensity data were recorded at temperatures 20, 38, 47, 56, and 63°C, employing a constant temperature device for Mark capillaries. The device is a single electronic temperature-control system which can control selectively for tem-

perature between 0 and 70°C and can be both cooled and heated using a Peltier element. Nylon 6 textile fibers of denier values (15/1), (18/1) and (20/1) were obtained from the Sir Padampat Research Institute, J.K. Synthetics, Kota, Rajasthan, India, for this study.

Porod⁸ introduced the invariant of the scattering curve which is given by the relation

$$Q_{\text{Expt}} = \int_0^{\infty} I(x)x^2 dx$$

where I is the desmeared intensity (Fig. 1),

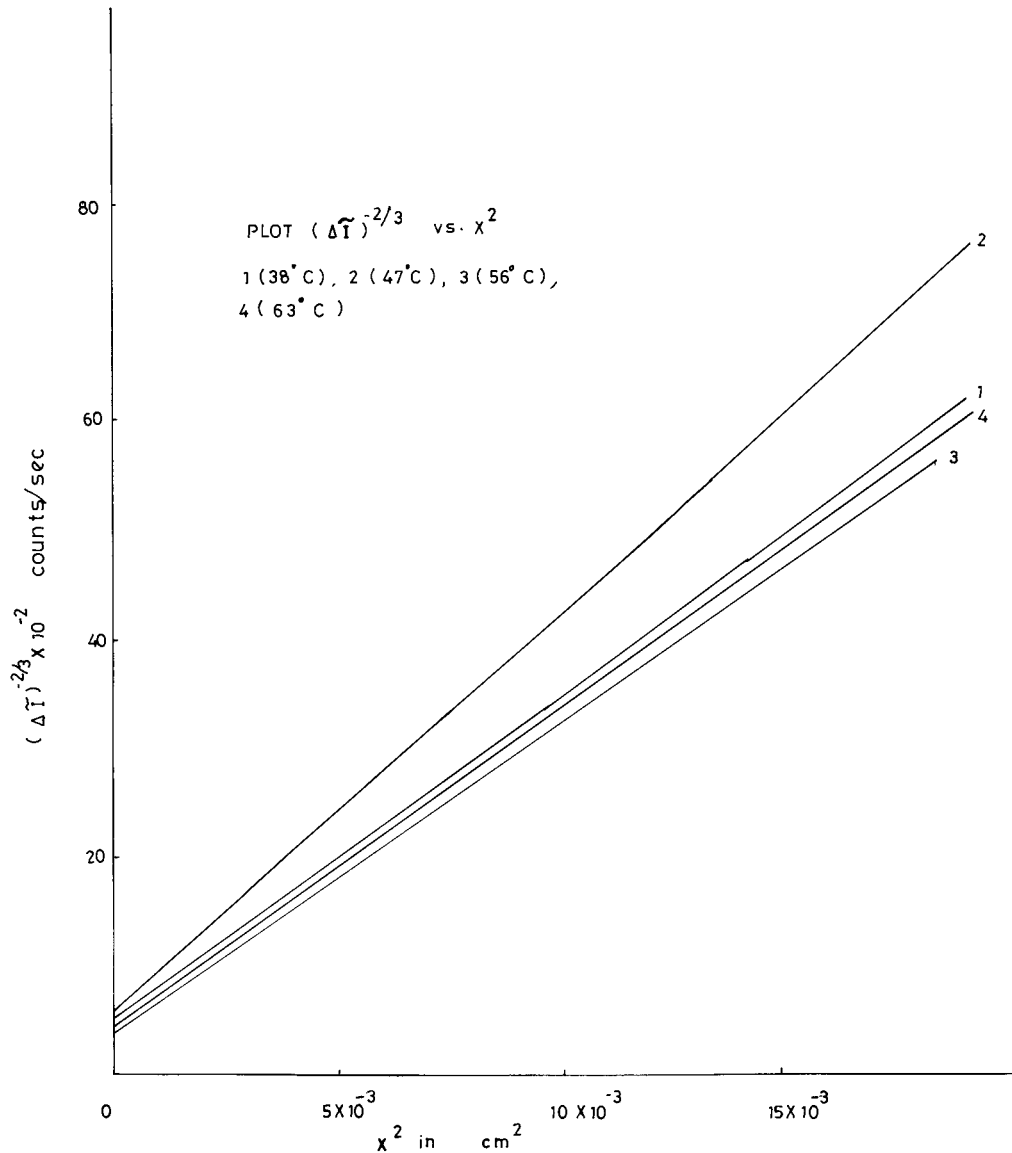


Figure 4 Smeared intensities (microvoid).

whereas

$$Q_{Th} = 1/4 \pi \cdot (e^2/mc^2)^2 \lambda^3 N^2 P_0 D a \rho^2 w_1 w_2$$

after Kratky,¹² where w_1 and w_2 are the volume fractions of the void and matter, respectively; e , the electronic charge; m , the mass of the electron; c , the velocity of light; λ , the X-ray wavelength ($= 1.54 \text{ \AA}$); N , the Avogadro number; D , the effective sample thickness; P_0 , the intensity of the primary beam of the X-ray; a , the countersample distance; and ρ , the electron-density difference of the scattering particles. Q_{Th} = the equation as per the literature and Q stands for the invariant. The value of the invariant is a

quantity independent of shape and size of the scattering parameters, but is dependent on the volume of the scattering particles. By equating Q_{Expt} with Q_{Th} , the value of void fraction w_1 may be determined since $w_2 \approx 1$.

Specific Inner Surface

The specific inner surface which is defined as the phase boundary area per unit volume of the dispersed phase is given after Kratky⁹ by

$$O/V = (2\pi^2/\lambda a) w_1 w_2 (K_1/Q)$$

for the desmeared intensity. The plot $I(x)x^4$ vs. x

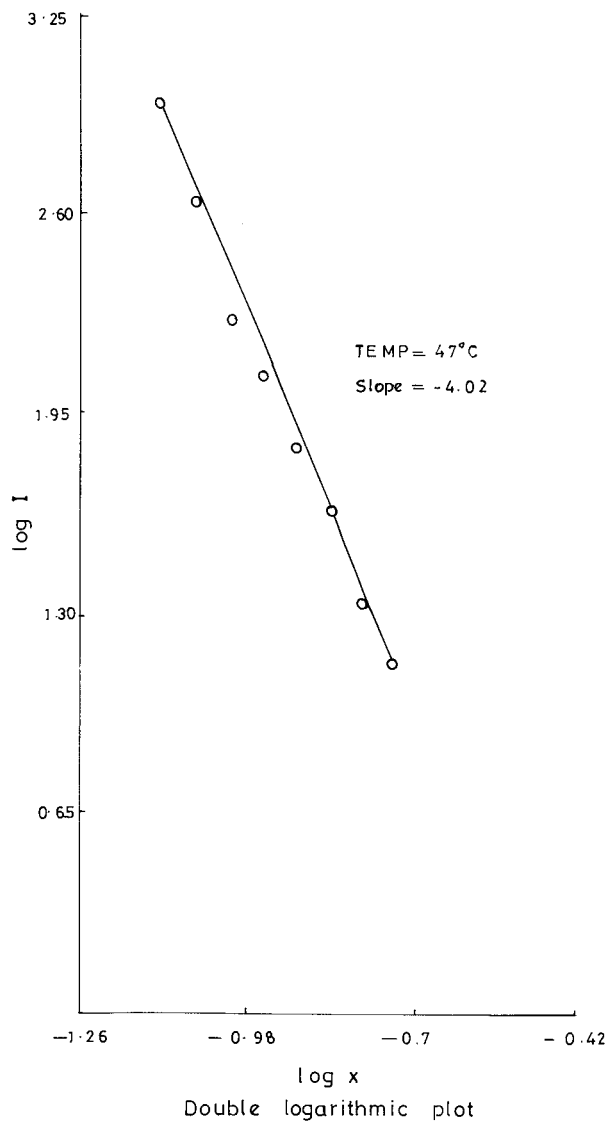


Figure 5 Double logarithmic plot.

(Fig. 2) yields the incoherent background scattering K_2 from the slope of curve and K_1 is the run constant.

Transverse Lengths

According to Kirste and Porod,¹³ the chord lengths of the arrows in all possible directions in the void and matter contained in the sample are given by

$$l_1 = 4w_1/(O/V) \quad \text{and} \quad l_2 = 4w_2/(O/V)$$

The Coherence Length

The coherence length l_c , introduced by Porod,⁸ also called the heterogeneity distance, is given by

$$I_c = \frac{(\lambda a/2) \int_0^\infty I(x) x dx}{\int_0^\infty I(x) x^2 dx} = (\lambda a/2) \cdot (\bar{E}/Q)$$

for the desmeared intensity, where $\bar{E} = \int_0^\infty I(x) x dx$ is the integrated scattering energy (Fig. 3).

The Microvoid Dimension

Microvoids were created in polyoxymethylene samples using the method of Wendorff.¹⁴ In the case of a continuous vibrational state, it was found that the average shape and size of microvoids approximates rotational ellipsoids. The small axis of the ellipsoid, the axis of rotation, coincides with the draw direction. The distribution of the size of the microvoids can be represented by an exponential density correlation function $C(r)$:

$$C(r) = \langle \delta\eta(x) \cdot \delta\eta(x+r) \rangle / \delta\eta(x)^2 \\ = \exp(-r/a)$$

x and $(x+r)$ are two locations separated by a distance r within the sample containing microvoids. $\delta\eta(x)$ represents the electron density difference between the microvoid and the polymer matrix. The average size of the microvoid d is related to the correlation length¹⁵ " a " by

$$d = a(1 - \nu)$$

where ν is the volume fraction of the microvoids. Thus, d is given approximately by the value of the correlation length for small values of ν .

The excess scattering $\Delta\tilde{I}$ for smeared intensities, which is the difference between the scattering curve at room temperature and at any other temperature of the sample, was analyzed in terms of particle scattering, since it was found to decrease continuously with the increasing scattering vector S where $S = 4\pi \sin \theta/\lambda$, 2θ being the scattering angle, and λ , the wavelength of X-radiation. The scattering can be described on the basis of the electron-density correlation function $C(r)$ as discussed earlier. Therefore,

$$\Delta\tilde{I}(s) = I_e V \langle \delta\eta(x^2) \rangle 4\pi a^2 / (1 + a^2 s^2)^{3/2}$$

where I_e is the scattering by an electron, and V , the scattering volume. The correlation length a , characterizing the average diameter of the particles, can thus be obtained from the slope and intercept of a plot of $\Delta\tilde{I}^{-2/3}$ vs. s^2 (Fig. 4), which should yield a straight line.

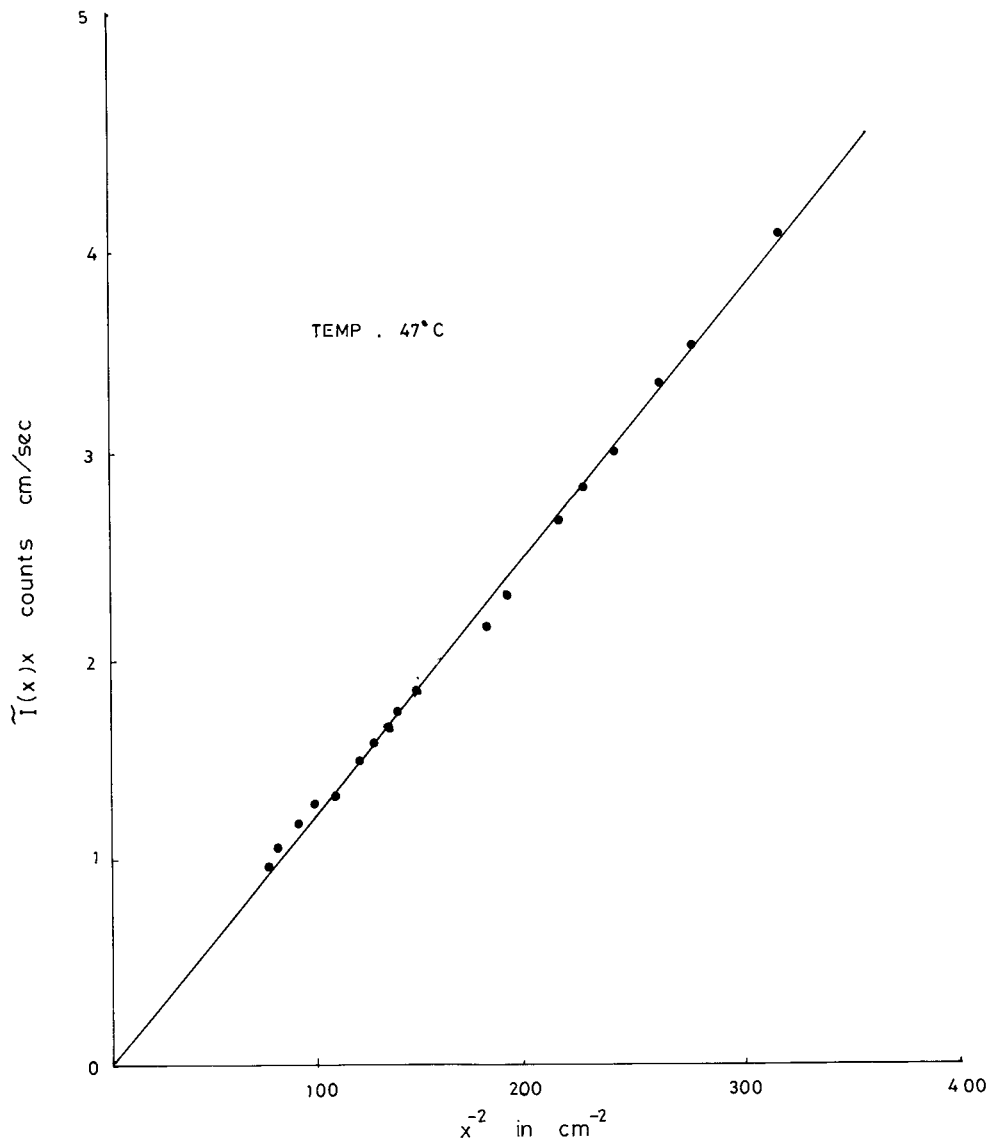


Figure 6 Ruland plot for transition layer ϵ for smeared intensity \tilde{I} .

RESULTS AND DISCUSSION

That the sample is a densely packed two-phase system with sharp boundaries was examined by the double logarithmic plot in which the slope of the curve was found to be -4 (Fig. 5) after Porod.⁸ Besides, in the Ruland¹⁶ plot between $\tilde{I}(x)x$ vs. X^{-2} , the curve passes through the origin without any intercept, thereby confirming the value of $\epsilon = 0$ (Fig. 6), where ϵ is the width of transition layer.

The intensities were normalized by bringing the intensities to the same value of a and d . The different normalized invariant curves plotted ($\bar{I}x^2$ vs. x) (Fig. 1) reveal a gradual increase in the values of Q with increasing temperature to 56°C ,

beyond which they decrease (Table I). The invariant Q is independent of the shape and size of the scattering particles and depends upon the total volume of the dispersed phase.¹⁷ The increase in the value of Q with the increase in temperature may be attributed to the phenomenon of swelling of the scattering particles, and the subsequent tendency to decrease beyond 56°C is due to the fragmentation of the swelled particles as it crosses the glass transition temperature. Beyond the glass transition temperature, the molecular motion sets in the crystalline region, thereby making it more amorphous, which is in agreement with the decrease in the value of Q . The gradual increase in the value of Q causes a decrease of the crystallinity of the sample; therefore, the tensile

Table I Comparison of Results

Parameters	Temperatures °C				
	20	38	47	56	63
(W_1)					
Void (%) $\times 10^{-2}$	0.015	0.018	0.02	0.021	0.023
(O/V)					
$\times 10^{-6} \text{ A}^{-1}$	0.92	3.214	2.72	3.02	3.185
l_1					
(A°)	652.0	225.0	294.0	280.8	289.0
l_2					
$\times 10^3 (\text{A}^\circ)$	4444.0	1244.0	1470.0	1324.0	1256.0
l_c					
(A°)	455.1	480.5	510.5	492.8	486.0
d					
(A°)	—	62.5	65.14	70.55	66.47
Q	0.171	0.234	0.267	0.281	0.274

quality of the Nylon 6 fiber is degraded. A comparative study of parameters with different denier values reveal that the invariant Q (Table II) also increases. Increasing denier values thereby imply the fact that crystallinity decreases for thicker filaments.

As Nylon 6 belongs to a group of semicrystalline polymers, the studies reveal the presence of microvoids along with the matter phase of the filament. The value of the microvoid dimension increases with increase of the temperature until 56°C (Fig. 4). At higher temperatures above 56°C, i.e., beyond the glass transition temperature, there is a tendency of a decrease in its value, the behavior having a correlation with the characteristics of the invariant Q at different temperatures.

Table II Comparison of Results at Different Denier Values at Temperature 20°C

Parameters	Denier/Filament		
	(15/1)	(18/1)	(20/1)
(W_1)			
Void (%) $\times 10^{-2}$	0.015	0.034	0.051
(O/V)			
$\times 10^{-6} \text{ A}^{-1}$	0.92	4.87	4.90
l_1			
(A°)	652.0	279.0	418.0
l_2			
$\times 10^3 (\text{A}^\circ)$	4444.0	829.8	816.0
l_c			
(A°)	455.1	412.6	518.8
Q	0.171	0.411	0.730

A comparative study of other parameters, like void percentage, length of coherence, specific inner surface, and transverse lengths at different temperatures of 20, 38, 47, 56, and 63°C for the filament of a denier value of (15/1) are recorded (Table I). A comparison was also made with denier values of (15/1), (18/1), and (20/1) at a temperature of 20°C (Table II).

REFERENCES

1. P. Debye and A. M. Bueche, *J. Appl. Phys.*, **20**, 518 (1949).
2. P. Debye and A. M. Bueche, *Theoretical and Applied Colloid Chemistry*, Vol. 7, Reinhold, New York, 1950.
3. H. M. Barton, *Phys. Rev.*, **79**, 211 (1950).
4. G. H. Vineyard, *Phys. Rev.*, **74**, 1076 (1948).
5. O. Kratky, *Progr. Biophys.* **13**, 107 (1963).
6. Y. Kawahara, *Nippon Sanshigaku Zasshi*, **62**, 234 (1993).
7. T. Mishra, T. Patel, A. K. Sahoo, N. Khan, and V. Buch, *Ind. J. Phys.* **67A**, 237 (1993).
8. G. Porod, *Kolloid Z.*, **124**, 83 (1951); **125**, 51 (1952).
9. O. Kratky, *Pure Appl. Chem.*, **12**, 483 (1966).
10. J. H. Wendorff, *Polymer*, **21**, 553 (1980).
11. O. Kratky and Z. Skala, *Z. Elektrochem.*, **62**, 73 (1958).
12. O. Kratky, G. Porod, A. Sekora, and B. Paletta, *J. Polym. Sci.*, **16**, 163 (1955).
13. R. Kirste and G. Porod, *Kolloid Z.Z. Polym.*, **184**, 1 (1962).
14. J. H. Wendorff, *Prog. Colloid Polym. Sci.*, **66**, 135 (1979).
15. P. Debye, *Z. Phys.* **156**, 256 (1959).
16. W. Ruland, *Appl. Cryst.*, **4**, 70 (1973).
17. T. Mishra, Dissertation of Ph.D. Thesis (1973).